Palaeogeography, Palaeoclimatology, Palaeoecology 292 (2010) 155–167

Contents lists available at ScienceDirect

Palaeogeography, Palaeoclimatology, Palaeoecology

journal homepage: www.elsevier.com/locate/palaeo

Chronology and integrated stratigraphy of the Miocene Sinj Basin (Dinaride Lake System, Croatia)

A. de Leeuw [a,*], O. Mandic [b], A. Vranjković [c], D. Pavelić [c], M. Harzhauser [b], W. Krijgsman [a], K.F. Kuiper [d]

[a] Paleomagnetic Laboratory "Fort Hoofddijk", Utrecht University, Budapestlaan 4, 3584 CD Utrecht, The Netherlands
[b] Geological–Paleontological Department, Natural History Museum Vienna, Burgring 7, 1010 Wien, Austria
[c] Faculty of Mining, Geology and Petroleum Engineering, University of Zagreb, HR-10000 Zagreb, Pierottijeva 6, P.O. Box 679, Croatia
[d] Isotope Geochemistry, Vrije Universiteit Amsterdam, De Boelelaan 1085, 1081 HV Amsterdam, The Netherlands

ARTICLE INFO

Article history:
Received 23 September 2009
Received in revised form 15 March 2010
Accepted 17 March 2010
Available online 21 March 2010

Keywords:
Chronology
Lacustrine sediments
Magnetostratigraphy
$^{40}Ar/^{39}Ar$ dating
Mollusk evolution
Conohyus

ABSTRACT

In the Miocene, the intra-montane basins of the Dinaric Mountain Chain harbored a series of long-lived lakes constituting the so-called Dinaride Lake System. The thick lacustrine sedimentary records of these lakes provide an excellent opportunity to study evolution and radiation of mollusks in an isolated environment. The 500 m thick infill that accumulated in the Sinj Basin is one of the key records because of its excellent mollusk preservation. Recent studies on the depositional history, pollen assemblages and large mammals have enhanced the understanding not only of Lake Sinj, but also of the regional climatic developments and faunal migratory patterns.

A reliable chronology of the development of Lake Sinj, which is crucial for global correlation of its endemic realm, was still lacking. In this paper we present a detailed time-frame for the Miocene Sinj basin based on palaeomagnetic and $^{40}Ar/^{39}Ar$ data. We conclude that deposition took place between 18.0 to 15.0 Ma, a time span that correlates with the upper Burdigalian and lower Langhian Mediterranean stages and Ottnangian, Karpatian and lowermost Badenian Paratethys stages. Furthermore, we determined the timing of several events in mollusk evolution, important for correlation across the Dinarides. An age of 15.0 Ma is attributed to the large mammals *Conohyus* and *Gomphotherium*, preserved in the upper part of the basin stratigraphy.

1. Introduction

During the Neogene, a series of lakes occupied many of the tectonic depressions in the Dinarides (Rasser et al., 2008). The strictly endemic nature of the aquatic fauna preserved in the lacustrine deposits of the Dinaride Lake System (Krstić et al., 2001, 2003; Harzhauser and Mandic, 2008) has up to now prevented a reliable correlation with the global time scale (Pavelić, 2002; Jiménez-Moreno et al., 2008). This hampered regional palaeogeographic reconstructions and comparison to the Mediterranean as well as Paratethys realms. This is unfortunate since the Dinaric–Anatolian land occupied a crucial position between the Mediterranean and Paratethys and potentially acted as a land bridge for mammal migration between Africa and Europe.

The lacustrine sediments of the Sinj Basin are particularly interesting because of their palaeontology. The thick lacustrine series contains a remarkably well preserved mollusk fauna (e.g. Brusina, 1874, 1897, 1902), providing an excellent opportunity to study evolution in an isolated system. Moreover, lignite deposits intercalated with the lacustrine series have provided an interesting vertebrate fauna with remains of the ancient pig *Conohyus* as well as the elephant ancestor *Gomphotherium* at the top of the Lučane section (Olujić, 1999; Bernor et al., 2004) and the rhinocerotid *Brachypotherium* at presumably slightly higher stratigraphic position in the coal layers of Ruduša NW of Sinj (Takšić, 1968). Although the thickness of the sedimentary succession suggests Lake Sinj was long-lived, *i.e.* persisted more than 100 kyr following classification by Gorthner (1994), the strictly endemic character of its fauna inhibits straightforward biostratigraphic estimation of the age and longevity and therefore calls for an independent age estimate.

In this paper we present the results of an integrated $^{40}Ar/^{39}Ar$ and magnetostratigraphic study of the calcareous lacustrine sediments of the Sinj Basin (Fig. 1). For this purpose, we selected the Lučane section in the western part of the basin (Figs. 2, 3). The Sinj Basin thereby becomes the first lacustrine basin in the Dinarides of which the age is reliably constrained. The chronostratigraphic results were constructed in a joint research effort and will be directly integrated with the simultaneously acquired palaeontological results.

2. Geological setting, paleogeography and basin stratigraphy

The geological setting of the Sinj Basin and the upper part of the Lučane section in particular were described in detail by Mandic et al.

* Corresponding author. Fax: +31 30 253 1677.
E-mail addresses: adeleeuw@geo.uu.nl (A. de Leeuw), oleg.mandic@nhm-wien.ac.at (O. Mandic), dpavelic@rgn.hr (D. Pavelić), klaudia.kuiper@falw.vu.nl (K.F. Kuiper).

0031-0182/$ – see front matter © 2010 Elsevier B.V. All rights reserved.
doi:10.1016/j.palaeo.2010.03.040

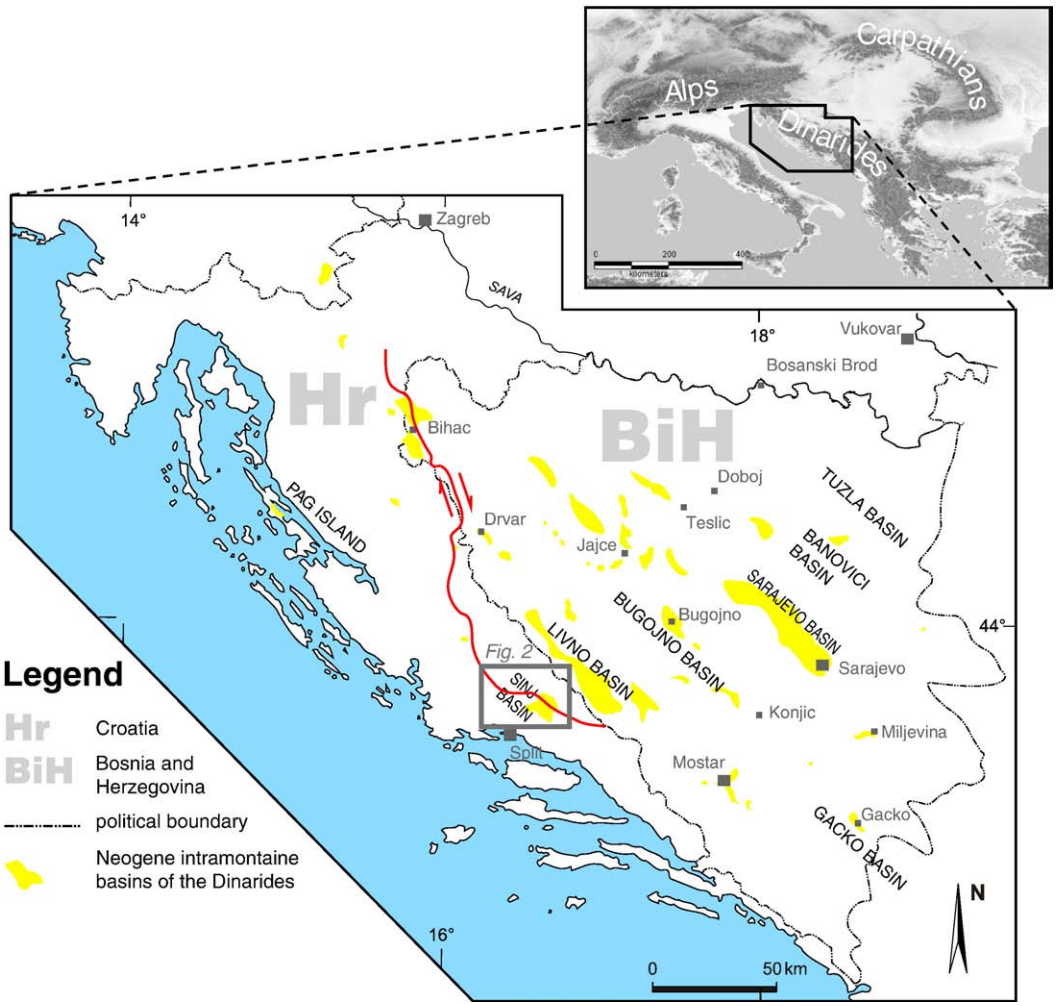

Fig. 1. Overview map showing the main Neogene basins within the Dinarids. The location of the Sinj Basin is highlighted within the grey frame. Hr: Croatia, BiH: Bosnia and Herzegovina. (Modified after Pavelić, 2002).

(2009) and Jiménez-Moreno et al. (2008). Here, a summary is given, with special emphasis on facts important for the chronostratigraphy.

The Sinj basin is situated in southeastern Croatia, in the western marginal part of the Dinaric Thrust Belt. The main phases of thrusting in this area occurred in the Middle and Late Eocene to possibly earliest Oligocene (Tari-Kovačić, 1994) and involved mainly Mesozoic to early Cenozoic limestones from the Adriatic–Dinaric Carbonate Platform. These thrust sheets eventually formed the basement for the Sinj Basin, which started to develop in the early Miocene. The Sinj basin is situated along the major Split-Karlovac Fault that crosscuts the Dinarides (Schmid et al., 2008; Tari-Kovačić, 2002). Basin evolution is controlled by strike–slip movement on the fault and the main decollement level is formed by Permo-Triassic pelitic and evaporite rocks.

The basin was mapped in detail by Kerner (1905b, 1916a,b), Marinčić et al. (1969,1977), Šušnjara and Ščavničar (1974), Raić et al. (1984), Papeš et al. (1982) and Šušnjara and Sakač (1988) and has a rhomboidal shape. The infill can be subdivided into 3 units: a lower unit with freshwater limestone and considerable terrigenous input, authigenic carbonate in the middle unit and carbonate with coal intercalations in the upper unit (Šušnjara and Sakač 1988) (Fig. 2). The main, 4 m thick, coal seam was formerly mined and it was from this layer that the large mammal fauna was collected (Olujić, 1999). Carbonates developed throughout the whole basin. Breccia intercalations in the upper part of the succession, located near the basin margins, point out the original relief (Mandic et al., 2009).

From the results of Mandic et al. (2009) and Jiménez-Moreno et al. (2008) it is clear that Lake Sinj was a carbonate hard water lake in a karst environment. Authigenic carbonate production prevailed and due to a flat morphology most of the lake remained in the photic zone. Periodically, perennial increases in water level occurred and at times the lake suffered acidification. Pollen records show that humid and colder climatic phases coincided with the deposition of limestone while arid and warmer phases provided coals.

Palaeobiogeographically, Lake Sinj belonged to the Dinaride Lake System (DLS). This long lasting and complex system generated a locally very thick infill in the intra-montane basins of the Dinarides (Krstić et al., 2001, 2003; Mandic et al., 2009; Pavelić, 2002; Rasser et al., 2008). In the Sinj Basin, sediment thickness comprises ~500 m (Fig. 4), while in the adjacent Livno basin the thickness reaches up to 2 km. Although its thick sedimentary succession and great species richness hint at longevity, accurate age constraints are lacking.

A rough age indication of the Sinj succession can be derived from its large mammal fauna represented by *Gomphoterium angustidens*, *Conochyus olujici* and *Brachypotherium brachypus*. These indicate a latest early Miocene to earliest late Miocene age (Mandic et al., 2009, Pálfy et al., 2007). *C. olujici* has been described as a new species on the basis of eight mandibular specimens, by Bernor et al. (2004). Their cladistic analysis suggests it is an early member of the clade. Such evolutionary stage inference for *C. olujici* led Bernor et al. (2004) to estimate the age of the topmost coal layer between 17 Ma and 16.1 Ma. The lower part of the Lake Sinj deposits contain

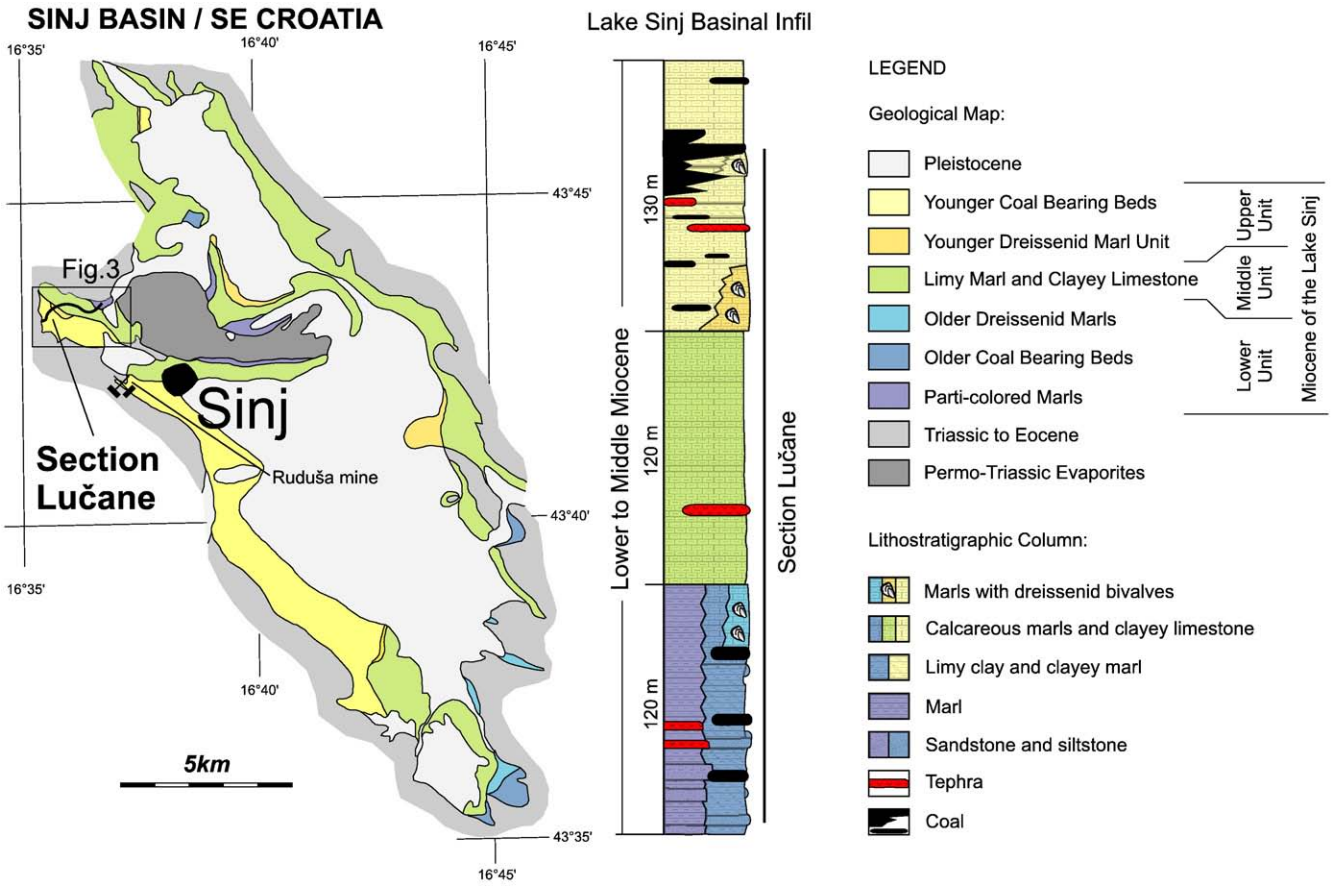

Fig. 2. Geological map and generalized stratigraphic column of the Sinj Basin (modified after Jiménez-Moreno et al. 2008). Subdivision and lithostratigraphic units according to Šušnjara and Sakač, 1988.

abundant *Doderleinia sinjana* (Kerner, 1905a) (cf. Jiménez-Moreno et al., 2008). While this plant is rare elsewhere, it is abundant in an early Miocene horizon in NE Austria and SW Czech Republic, which corresponds to the late Ottnangian (app. 17.5 Ma after Rögl et al., 2004).

3. The Lučane section: lithostratigraphy, biostratigraphy and earlier works

The studied Lučane section is located in the westernmost part of the Sinj Basin. Although Mandic et al. (2009) and Jiménez-Moreno

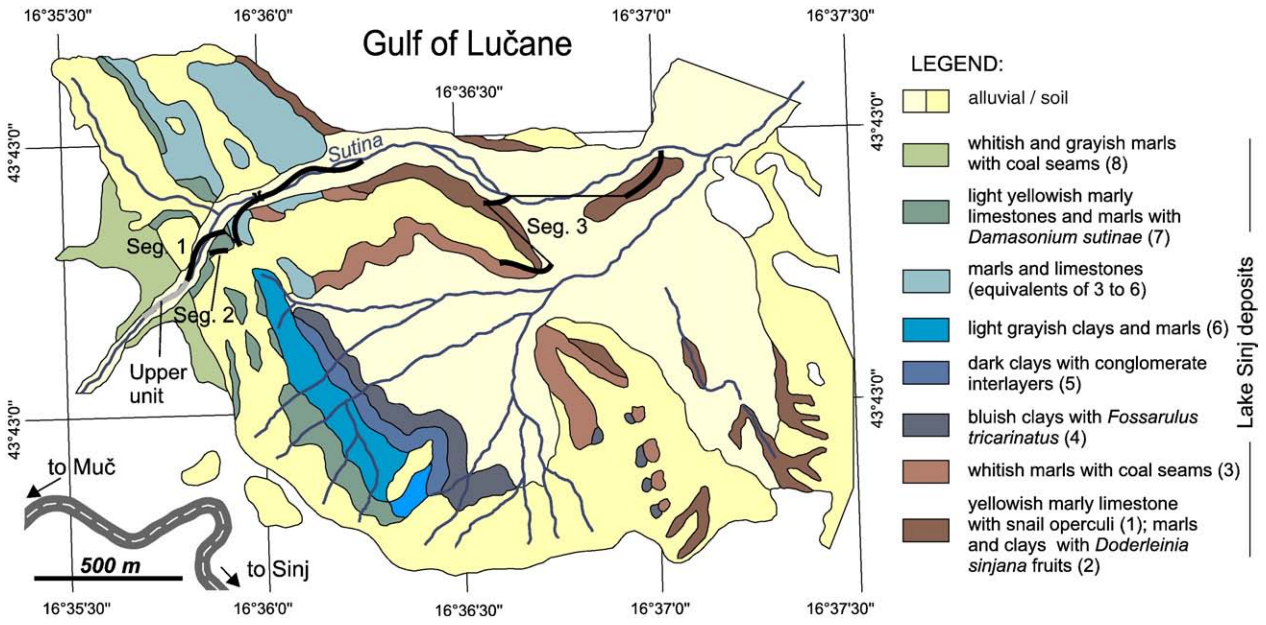

Fig. 3. Detailed geological map of the Lučane area, located in the western part of the Sinj Basin. (Modified after Kerner 1905b) The traces of the individual segments of the studied section are indicated.

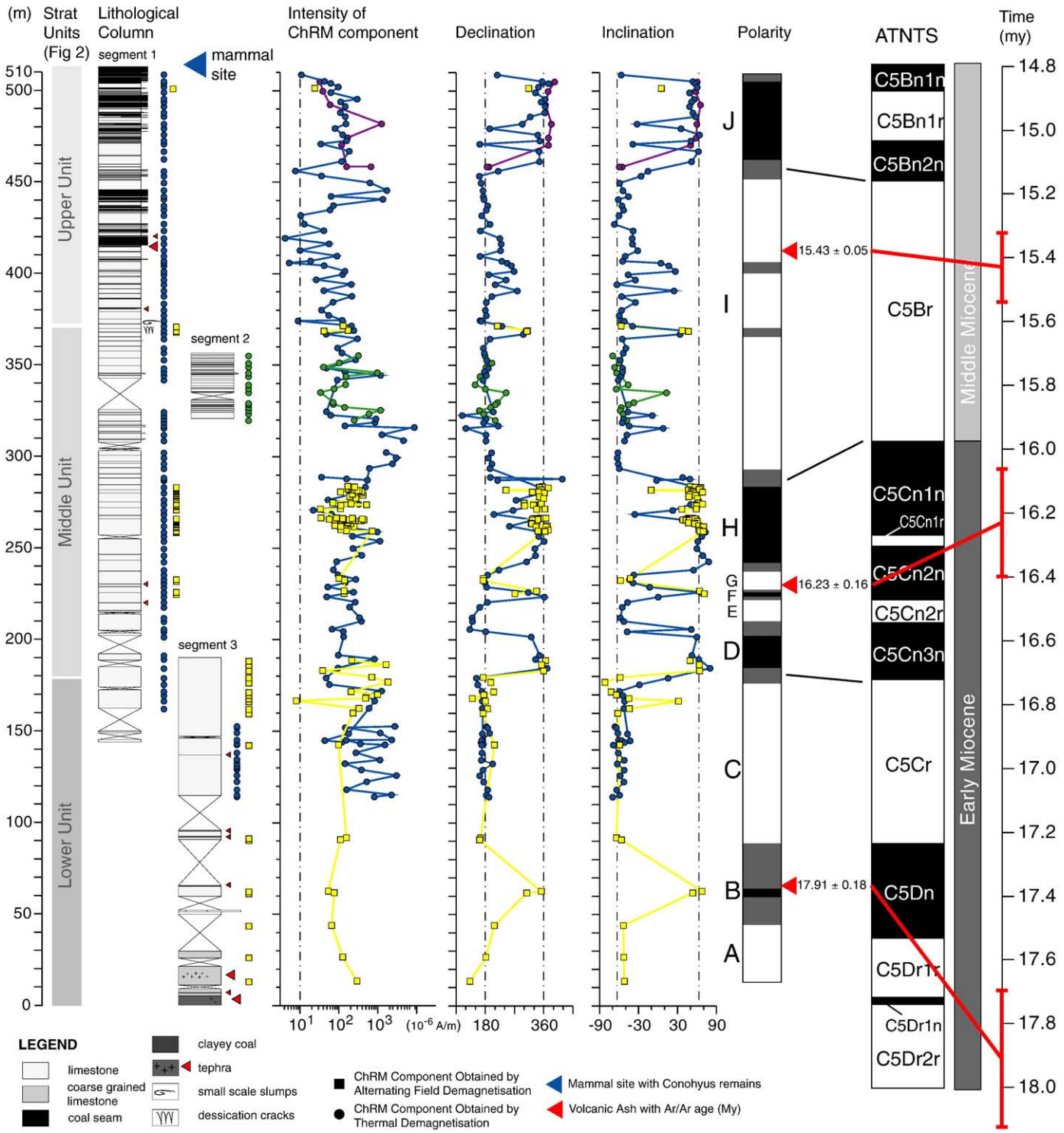

Fig. 4. Lithological column, fossil distribution and magnetic results for the Lučane section. The polarity pattern derived is correlated to the ATNTS using the $^{40}Ar/^{39}Ar$ ages as primary tie points. ATNTS according to Lourens et al., 2004 with adjustments by Hüsing 2008.

et al. (2008) described only the uppermost coal bearing unit, all three (Fig. 2) lithological units defined by Šušnjara and Šćavničar, (1974) are reflected in this section and were sampled for magnetostratigraphy (Fig. 4). Several volcanic tuffs intercalate with the lacustrine limestone. The most prominent tuff is located at the section base i.e. at the base of the lowermost of the three units. The most fossiliferous part of the section is found in its upper unit.

Mollusk preservation as well as species richness provides the Sinj Basin with a high potential for the study of isolated evolution (Harzhauser and Mandic, 2008, 2010). The amount of species described is one of the highest in the Dinaride Lakes and might be partially influenced by the exceptional faunal preservation in some of its classic localities (Brusina, 1884). The taxonomic content of the Lučane mollusk fauna was referred to by Brusina (1884, 1897), Kerner (1905b), Kittl (1895), Olujić (1936, 1999), and Mandic et al. (2009). Compared to other mollusk localities in Sinj, the Gulf of Lučane shows rather moderate fossil preservation. Yet, as pointed out by Kerner (1905b), due to good outcrop conditions, showing the most complete

and well exposed lacustrine succession in the Sinj Basin, it is certainly the best place for a relational study on the biotic and palaeoenvironmental evolution in this palaeolake. Several distinct evolutionary lines from the upper limestone and coal bearing unit were already described by Olujić (1936, 1999). This stratigraphic interval also records the late stage optimum of *Mytilopsis* evolution in the DLS. As postulated by Kochansky-Devidé and Slišković (1978) this implies the biostratigraphic correlation of the topmost Lake Sinj infill with the youngest sediments of the DLS elsewhere.

While the fossil content and lithology of the uppermost unit in the Lučane section was described in detail by Mandic et al. (2009), the lower- and middle unit deserve a short description here. The Lučane section is a composite, built up from three partially overlapping segments (Fig. 4), not to be confused with the three units defined in Fig. 2. While the upper- and middle unit (Fig. 2) are very well exposed along the Lučane river valley, the lower unit crops out in a meadow and several parts remain unexposed. This could be related to a considerable amount of terrigenous input in this unit, the marly facies being more prone to erosion. At the base of this unit, a prominent, several meters thick, layer of volcanic origin crops out. Above it, between 8 and 100 m, dominantly coarser grained limestones surface. The almost complete lack of fossils hints at post-depositional leaching, which is supported by the presence of operculi of *Bythinia* around 28 m and *Mytilopsis hercegovinensis* coquina around 65 m. Several thin, mostly benthonized tuff layers occur in this interval. Furthermore, intercalations of breccia-conglomerate could indicate sporadic fluvial and/or debris flow influence. The lime mudstone dominating the interval consists of very fine-grained micrites. The deposition of the fine-grained components of lacustrine carbonates is dominantly induced by photosynthetic activity of macrophytes and microphytes and is characteristic for deeper and protected lake parts.

From approximately 100 m upward, exposure and fossil preservation are better. The sediments consist mainly of limestone and *Mytilopsis jadrovi*, *M. hercegovinensis*, *Melanopsis bicoronatus, Fossarulus tricarinatus, Orygoceras dentaliforme* and *Doderleinia* fruits are common in its lower part and *M. drvarensis* in its upper part. These limestones are usually light-colored, thin to medium bedded, and commonly soft and porous. They primarily consist of calcite and its $CaCO_3$ content reaches up to 99%. The dominating facies types are: detrital limestone generated from redeposited clastic material of older lacustrine and/or palustrine deposits exposed on mud flats, charophycean mudstone or wackstone with rooted submerged macrophytes indicating vegetated littoral environments, stromatolite bindstone consisting of alternating thin micritic laminae, or alternatively micrite to microsparite laminae both containing micrite-calcified microbial filaments, and finally mollusk wackstone with coquinas. The latter ones suggest a calm, very shallow freshwater environment prone to occasional storm events. The interval correlates with the units 2 to 7 of Kerner (1905b).

Jiménez-Moreno et al. (2008) made a detailed analysis of the pollen spectra along the topmost 100 m of the Lučane section. They distinguished four plant ecosystems in the pollen data. Those are a swamp and riparian environment, a broad-leaved evergreen forest (sea level — 700 m in altitude), an evergreen and deciduous mixed forest (>700 m) and finally a mid-altitude deciduous and coniferous mixed forest (>1000 m). Surprising is the high abundance of *Engelhardia* and the low presence of *Taxodium*-type and *Quercus*-type in comparison with other studies from Croatia, Central and Western Europe. These results also show that periods characterized by thermophilous and xeric plants alternate with periods characterized by a high abundance of conifers. These changes in the section's pollen spectra generally coincide with changes in the sedimentary regime. Increases in thermophilous and xeric pollen, likely indicating a warming-induced upslope displacement of broad-leaved evergreen forests, are generally associated with the frequent deposition of coal in the basin. This denotes periods of low lake levels and peat forming paludal swampy conditions. Peaks in pollen originating in the higher altitude conifer forest and simultaneous decreases in thermophilous pollen generally coincide with the deposition of deep littoral and organic-poor limestones. These periods denote a higher lake level and downslope displacement of the conifer vegetation belt in response to a colder climate.

4. Methods

4.1. Isotopic dating

Eleven volcanic ashes are intercalated with the limestone- and coal beds of the Lučane section. All of them were sampled for $^{40}Ar/^{39}Ar$ dating. The bulk samples were crushed, disintegrated in a dilute calgon solution, washed and sieved over a set of sieves between 63 and 500 μm. Only 3 of the 11 tephra samples contained potentially suitable minerals. Of each of the three suitable samples the largest appropriate mineral fraction was subjected to standard heavy liquid and magnetic separation techniques for sanidine as well as biotite. Samples Lučane 1, 2 and 3 held sanidine crystals in fractions 355–500 μm, 120–200 μm and 250–500 μm respectively. In addition, samples Lučane 1 and 3 contained biotite crystals in fractions larger than 355 and 400 μm respectively. All samples were subsequently handpicked. Sanidine separates were leached with a 1:5 HF solution in an ultrasonic bath during 5 min. Biotite separates were cleaned in an ultrasonic bath using pure demineralized water.

The mineral separates from Lučane 1 were loaded in a 6 mm ID quartz vial together with Fish Canyon Tuff (FC-2) and Drachenfels (Dra-1, f250–500) sanidine. Separates from Lučane 2 and 3 were put in a 9 mm ID quartz vial together with the same standards. Additional Drachenfels (Dra-2, $f>500$) sanidine was added to the latter vial as a third standard. Both vials were irradiated in the Oregon State University TRIGA reactor in the cadmium shielded CLICIT facility for 10 h.

Upon return to the VU Argon Laboratory, both standards and Lučane samples were pre-heated under vacuum using a heating stage and heat lamp to remove undesirable atmospheric argon. Thereafter, samples were placed in an Ultra High Vacuum sample chamber, degassed overnight and were either fused or incrementally heated using a Synrad CO_2 laser in combination with a Raylase scanhead as a beam delivery and beam diffuser system. After purification the resulting gas was analyzed with a Mass Analyzer Products LTD 215-50 noble gas mass spectrometer. Beam intensities were measured in a peak-jumping mode in 0.5 mass intervals over the mass range 40–35.5 on a Balzers 217 secondary electron multiplier. System blanks were measured every three to four steps. Mass discrimination was monitored by frequent analysis of aliquots of air. The irradiation parameter J for each unknown was determined by interpolation using a second-order polynomial fitting between the individually measured standards. All $^{40}Ar/^{39}Ar$ ages have been calculated with the ArArCalc software (Koppers, 2002) and applying the decay constants of Steiger and Jäger (1977). The age for the Fish Canyon Tuff sanidine flux monitor used in age calculations is 28.201 ± 0.03 My (Kuiper et al., 2008). The age for the Drachenfels sanidine flux monitor is 25.42 ± 0.03 My (Kuiper et al., in prep). Correction factors for neutron interference reactions are $2.64 \pm 0.017 \times 10^{-4}$ for $(^{36}Ar/^{37}Ar)_{Ca}$, $6.73 \pm 0.037 \times 10^{-4}$ for $(^{39}Ar/^{37}Ar)_{Ca}$, $1.211 \pm 0.003 \times 10^{-2}$ for $(^{38}Ar/^{39}Ar)_{K}$ and $8.6 \pm 0.7 \times 10^{-4}$ for $(^{40}Ar/^{39}Ar)_{K}$. Errors are quoted at the 1σ level and include the analytical error and the error in J.

4.2. Palaeomagnetism

Over 300 palaeomagnetic cores were taken along the 500 m thick Lučane section in 3 successive sampling campaigns. The gross resolution thus achieved was approximately one sample every 2 m. Only in the lower part of the section resolution remained lower due to

bad exposure and non-suitable lithologies. Samples were collected with a hand-held electric as well as gasoline-powered drill. The orientation of all samples was measured by means of a magnetic compass. Bedding planes were similarly determined at regular intervals.

In the laboratory, the obtained cores were cut into several specimens that were subsequently stepwise demagnetized. Samples from the earlier sampling campaign were all demagnetized thermally. Cores from the later campaigns were subjected to robotized alternating field (AF) demagnetization. Results were in good correspondence with those of thermal demagnetization. The natural remanent magnetization (NRM) of the samples was measured after each demagnetization step on a 2G Enterprises DC Squid cryogenic magnetometer (noise level $3 \cdot 10^{-12}$ A m^2). Heating occurred in a laboratory-built, magnetically shielded furnace employing 10–30 °C temperature increments up to 285 °C. AF demagnetization was accomplished by a laboratory-built automated measuring device applying 5–20 mT increments up to 100 mT by means of a degausser interfaced with the magnetometer. The characteristic remanent magnetisation (ChRM) was identified through assessment of decay-curves and vector end-point diagrams (Zijderveld, 1967). ChRM directions were calculated by principal component analysis (Kirschvink, 1980).

5. Results

5.1. Isotopic dating

The results of the $^{40}Ar/^{39}Ar$ total fusion experiments of the Sinj Lučane samples 1, 2 and 3 are given in Fig. 5 and Table 1. For Lučane 1 and 2, 10 multiple sanidine grain fusion experiments have been analyzed. We do not observe a homogeneous age population. However, based on the corresponding probability density distribution, we assume that those experiments comprising the youngest cluster contain no or only a negligible detrital component and represent a maximum crystallization age for the ash. We selected these experiments for calculation of the weighted mean age and error. For sample Lučane 1 the percentage radiogenic $^{40}Ar^*$ is on average 93%, which is relatively low for sanidine. The average radiogenic $^{40}Ar^*$ for sample Lučane 2 is 98%. The isochron ages are concordant with the weighted mean age and the trapped $^{40}Ar/^{36}Ar$ component is atmospheric. This provides and age of 15.43 ± 0.05 Ma for Lučane 1 and 16.23 ± 0.16 Ma for Lučane 2. The peak probability density age calculated based on all 10 experiments coincides exactly with the calculated weighted mean ages for both samples. Errors only slightly increase to respectively ± 0.054 Ma and ± 0.164 Ma when uncertainties for respectively the age of astronomically calibrated standard and decay constants, as reported in Kuiper et al. (2008) and Steiger and Jäger (1977) respectively, are included. This is a conservative error estimate including all sources of uncertainty. The largest part of the total uncertainty for these samples arises from the analytical uncertainty in *J*-values where we use a conservative approach. All relevant analytical data and an overview of the applied *J*-value calculations as well as error determination can be found in the online supplementary material. The age distributions as depicted in Fig. 5 are slightly heterogeneous due to the presence of a small fraction of reworked crystals in the samples.

For Lučane 3, initial analyses failed as indicated by the variable ages spanning a range between 17.5 and 40 Ma. Subsequent more thorough grain selection resulted in 5 additional analyses out of which three show K/Ca (30.5) and $^{40}Ar^*$ (99.3%) values attributable to sanidine and provide realistic ages. Based on the corresponding probability density distribution, two of the three experiments that cluster best were selected for calculation of the weighted mean age and related parameters. On the basis of these few data points a weighted mean age of 17.63 ± 0.18 Ma for the Lučane 3 sanidine can be calculated. Additional age information is provided by 10 additional experiments with multiple grain fusions of selected biotite crystals from the same sample. For these crystals, the average radiogenic $^{40}Ar^*$ amounts to 66% which is relatively low for biotite and might indicate slight weathering to chlorite. The weighted mean age of all 10 biotite fusion analysis yields 17.67 ± 0.20 Ma with a relatively high MWSD value of 6.7. But since these results hint at minor alteration of the biotite crystals it was decided to perform two incremental heating experiments on the same separate.

The results of the incremental heating experiments are presented as age spectra diagrams (Fig. 5). An age is accepted as an accurate estimate of the crystallization age when the following criteria are fulfilled. There should be a well-defined, high temperature plateau for more than 50% of the ^{39}Ar released formed by three or more concordant, contiguous steps. A well-defined isochron should be obtained from the results of the gas fractions on the plateau, while also the $^{40}Ar/^{36}Ar$ intercept for the trapped argon derived from the isochron should not be significantly different from the atmospheric ratio of 295.5 (McDougall and Harrison, 1999). Indeed, the age spectra diagrams for the first as well as the second incremental heating experiment show minor weathering along grain boundaries. After several heating increments, however, a well-defined plateau appears. For both experiments it comprises around 80% of the cumulative ^{39}Ar release and consists of 8 and 9 contiguous concordant steps. The respective weighted mean ages are 17.90 ± 0.18 Ma for the first and 17.93 ± 0.18 Ma for the second replication. The isochron ages correspond to the weighted mean ages (Table 1) and the trapped $^{40}Ar/^{36}Ar$ component is atmospheric. The total crystallization ages calculated using all incremental heating experiments indeed correspond to those found in the total fusion experiments. Since the incremental heating age spectra diagrams are well-defined and the use of the weighted mean plateau ages circumvents bias due to minor alterations, we take 17.92 ± 0.18 to represent the crystallization age of the Lučane 3 biotite crystals.

5.2. Palaeomagnetism

Thermal demagnetization diagrams indicate that the total NRM of the samples is generally composed of two components. Blocking spectra slightly overlap, as can be observed in Fig. 6a–g. The low temperature component is mostly removed at 220° and is interpreted to be an overprint. The NRM intensities after heating up to 220 °C typically range between 10^{-2} and 1.5 mA m^{-1}, as is common for limestones with a low detrital component. ChRM directions are generally established above this temperature and the component under consideration mostly decays straight to the origin. At 285 °C on average around 75% of the NRM is removed.

Samples subjected to AF demagnetization can be divided into two groups on the basis of the intensity of their NRM and corresponding ChRM. For the first group, in which samples generally have a higher intensity NRM, ChRM directions can be reliably established and have a starting intensity over 100 μA/m (Fig. 6h–j). For this group, the total NRM consists of two components. The first component, mostly removed at 20 mT, is interpreted to be an overprint. ChRM directions are established above 20 mT. For this group demagnetization diagrams display characteristics very similar to the thermal results and ChRM intensity also typically ranges between 10^{-2} and 1.5 mA m^{-1}. The second group of samples has a generally lower intensity NRM and

Fig. 5. Overview of the $^{40}Ar/^{39}Ar$ results. a) Probability density distribution for the multiple single fusion experiments on Lučane 1, 2 and 3 sanidine and Lučane 3 biotite. b) First incremental heating spectrum for Lučane 3 biotite. The chosen age plateau and corresponding weighted mean age are indicated. c) Second incremental heating spectrum for Lučane 3 biotite with chosen plateau and corresponding weighted mean age.

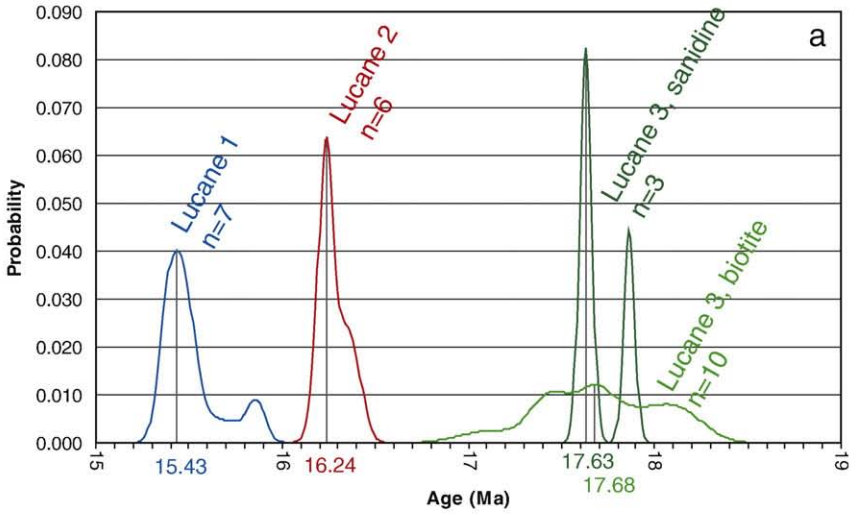
a
Probability
Lucane 1
n=7
Lucane 2
n=6
Lucane 3, sanidine
n=3
Lucane 3, biotite
n=10
15.43
16.24
17.63
17.68
Age (Ma)

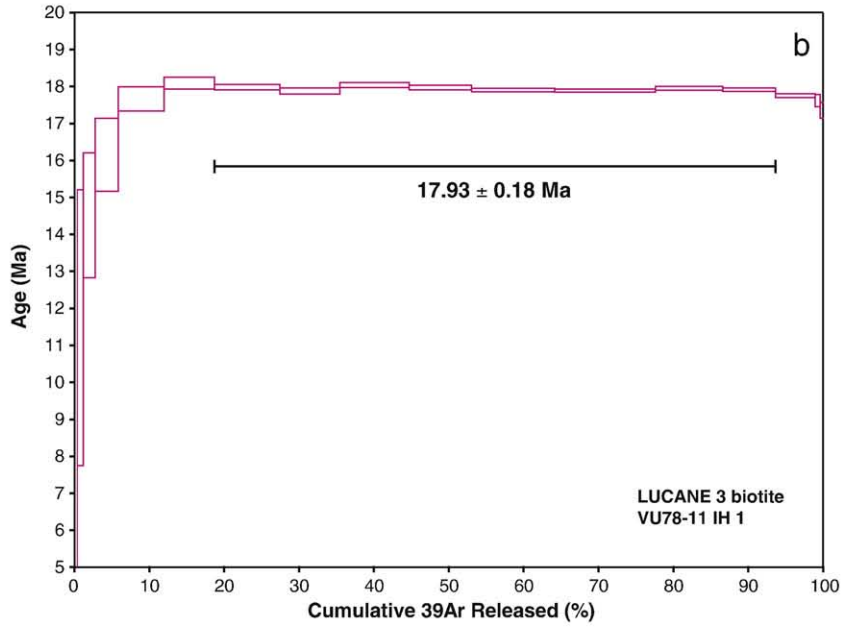
b
17.93 ± 0.18 Ma
LUCANE 3 biotite
VU78-11 IH 1
Age (Ma)
Cumulative 39Ar Released (%)

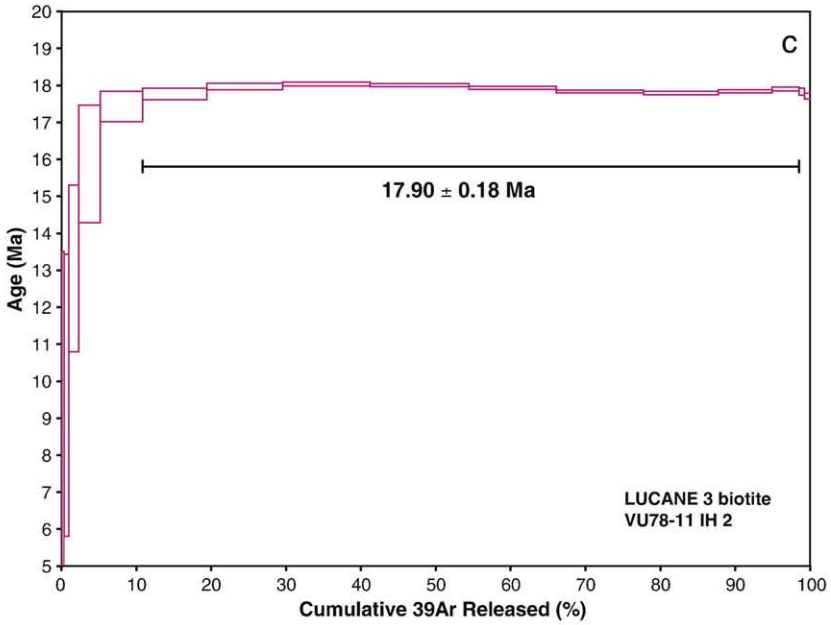
c
17.90 ± 0.18 Ma
LUCANE 3 biotite
VU78-11 IH 2
Age (Ma)
Cumulative 39Ar Released (%)

Table 1
Summary of the $^{40}Ar/^{39}Ar$ results. MSWD is Mean Square Weighted Deviates, *N* is the total number of repetitions in the single fusion experiments and the total number of steps in the incremental heating experiments. In brackets the number of experiments used to calculate the weighted mean or peak probability density age. $^{39}Ar_K$ is the percentage of $^{39}Ar_K$ released by plateau steps. ^{40}Ar is the radiogenic amount of ^{40}Ar. Total fusion and isochron ages and inverse isochron intercepts are given for reference. Errors are given at 95% confidence level. MSWD, $^{40}Ar^*$ (%), $^{39}Ar_K$ (%), K/Ca, Isochron age (Ma) and Inverse isochron intercept were determined based on the experiments selected for calculation of the weighted mean age.

Irradiation ID	Sample	Mineral	*J*-value	Peak probability density age (Ma)	Weighted mean age (Ma)	MSWD	*N*	$^{40}Ar^*$ (%)	K/Ca	Total fusion age (Ma)	Isochron age (Ma)	Inverse isochron intercept
VU69-C11	Lucane 1	Sanidine	0.0026093	15.43	15.43 ± 0.05	0.81	10(7)	93.18	10.09	15.52 ± 0.05	15.39 ± 0.09	305.5 ± 18.7
VU78-3	Lucane 2	Sanidine	0.002662	16.24	16.24 ± 0.05	0.05	10(6)	98.00	25.65	16.27 ± 0.05	16.24 ± 0.07	287.6 ± 43.1
VU78-1	Lucane 3	Sanidine	0.00266	17.62	17.63 ± 0.06	0.23	5(2)	99.24	60.25	17.92 ± 0.06	–	–
VU78-11	Lucane 3	Biotite	0.0026682	17.63	17.67 ± 0.11	6.69	10(10)	65.98	18.13	17.69 ± 0.7	17.05 ± 0.31	315.9 ± 10.2
Irradiation ID	Sample	Mineral	*J*-value	Plateau age (Ma)	MSWD	*N*	$^{40}Ar^*$ (%)	$^{39}Ar_K$ (%)	K/Ca	Total fusion age (Ma)	Isochron age (Ma)	Inverse isochron intercept
VU78-11-IH1	Lucane 3	Biotite	0.0026682	17.93 ± 0.18	0.78	18(8)	82.38	74.95	16.47	17.69 ± 0.18	17.92 ± 0.18	297.1 ± 2.7
VU78-11-IH2	Lucane 3	Biotite	0.0026682	17.90 ± 0.18	3.04	18(9)	85.02	87.26	6.71	17.65 ± 0.19	17.87 ± 0.18	298.2 ± 3.7

there is a large scatter observable in the demagnetization diagrams (Fig. 6l). If the NRM decayed below 100 μA/m after application of a 25 mT field, reliable ChRM directions could usually not be established.

No gyroremanence is observed even when applying alternating fields as large as 100 mT. At this field strength the remaining NRM of the majority of samples is negligible. The absence of gyroremanence and almost complete removal of the NRM at 80–100 mT suggests the most likely magnetic carrier is magnetite.

The directions isolated by means of principle component analysis as described above as well as the intensity of the ChRM are plotted against stratigraphic level in Fig. 4 in order to establish a magnetostratigraphy for the Lučane Section. NRM intensity does not correlate with lithology on a macroscopic scale. Potential correlation on a bed to bed scale was not investigated.

6. Discussion

6.1. Age model

The palaeomagnetic data gathered along the Lučane section allow establishing a reliable magnetostratigraphy for the infill of the Sinj Basin. Correlation of this magnetostratigraphy to the Astronomically Tuned Neogene Timescale (ATNTS) (Lourens et al., 2004), using the absolute ages of the three dated ash layers as tie points, is straightforward.

The age of the very top of the Sinj section is constrained by correlation of the uppermost normal interval to chron C5Bn.2n. with an astronomical age of 15.160 Ma (Lourens et al., 2004). While a single site suggests a transition from normal to reversed at the very top of the section, the large amount of organic material in that part obscures the palaeomagnetic signal. However, given the relatively thick upper normal magnetozone we can presume that the top of the section may well include, or be very close to, the C5Bn.2n to C5Bn.2r reversal boundary. In this way, we arrive at an age of 15.0 My for the top of the Lučane section.

The age of the base of the section is constrained by the $^{40}Ar/^{39}Ar$ age for the Lučane 3 tuff layer. Bad outcrop exposure resulted in a poor magnetostratigraphy for this part of the section and the age of 17.92 ± 0.18 Ma remains the only tie point. Accordingly, we arrive at an age of approximately 18 Ma for the base of the Lučane section.

The Lučane section was thus deposited from 18.0 to 15.0 Ma. It correlates to the upper Burdigalian and lower Langhian Mediterranean stages and Ottnangian, Karpatian and lowermost Badenian Paratethys stages. This period, except for its initial part, coincides largely with the Middle Miocene Climatic Optimum. Formation of Lake Sinj and accumulation of its thick limestone series might thus have been stimulated by the favourable climatic conditions.

It should be kept in mind that the ages of the reversal boundaries between C5Dr1r and C5Bn2n, to which the major part of the section is correlated, were determined on the basis of spreading rates in the ATNTS (Lourens et al., 2004). The ages of the reversal boundaries can easily turn out to be up to 40 ka off, once an astronomical tuning for this part of the Miocene will be established.

The misfit in the reversal pattern between polarity interval D and H most likely arises due to difficulties retrieving the original magnetic signal. It might, on the other hand, indicate the presence of a hiatus. Then the major part of chron C5Cn.2n could be lacking in the Lučane record. Direct field evidence for the presence of such hiatus was, however, not found. When compared to the astronomical time scale of Billups et al. (2004) the missfit within C5Cn is much smaller. It also shows a better fit with the magnetostratigraphic record of chron C5Cn in the Ebro Basin (Larrasoaña et al., 2006; Pérez-Rivarés et al., 2004) as well as deep sea IODP records (Lanci et al., 2004), where magnetozones corresponding to C5Cn.2r are always thicker than one would expect from its estimated duration in Lourens et al. (2004).

In the largest part of the section, the constructed magnetostratigraphy provides a good control on the sedimentation rate (Fig. 7). The lower half of the section has a sedimentation rate of approximately 10 cm/kyr while the upper half was deposited at the double rate of 20 cm/kyr. The sedimentation rates at the very top and bottom of the section do not deviate excessively from rates in the rest of the section. Incipient tectonism related to the start as well as the end of sedimentation in the Sinj Basin might however have caused the sedimentation rate to be temporarily higher.

6.2. Lithostratigraphy, fossil flora and climate change

Lithostratigraphic subdivision of the western part of the Sinj Basin by Kerner (1905b) is also based on changes in plant assemblages (Fig. 3). Equipped with the new age model we are now able to calibrate the lithostratigraphic units and biostratigraphic markers to the geological time scale. This allows correlations of the Lake Sinj plant assemblages with related occurrences outside the DLS.

The lower part of the studied succession (zone 2 according to Kerner, 1905b) is characterized by the common occurrence of conspicuous *Doderleinia* fruits (a tentative tape-grass representative, Jiménez-Moreno et al., 2008). This interval is now dated at ~17 Ma and thus correlates to the late Burdigalian (Fig. 8). This suggests that

Fig. 6. Thermal (th) and alternating field (af) tectonically corrected (tc) and tectonically non-corrected (notc) demagnetization diagrams for samples from the Lučane section. For an elaborate description we refer to the Results section.

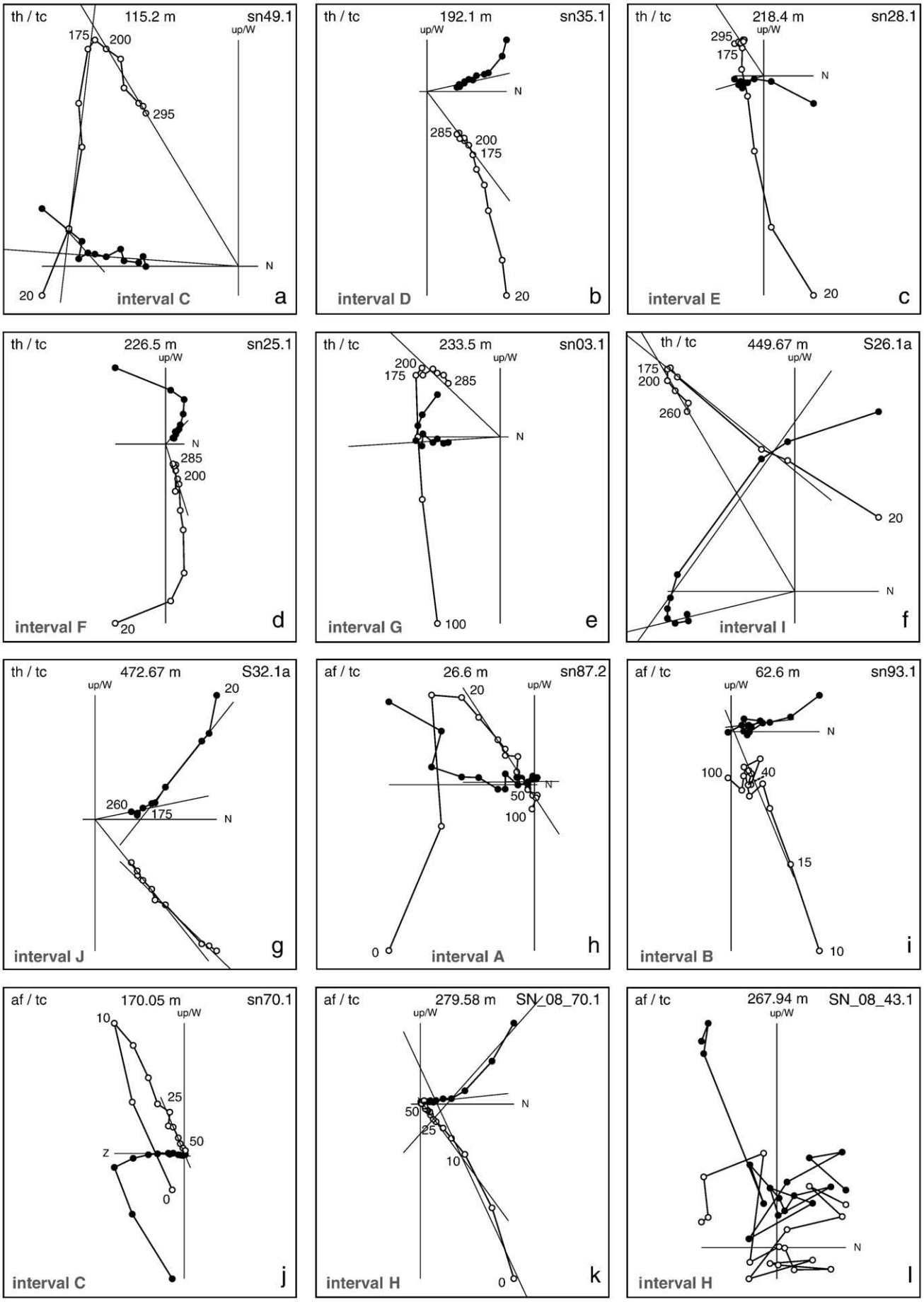
th / tc
115.2 m
sn49.1
up/W
175
200
295
N
20
interval C
a
th / tc
192.1 m
sn35.1
up/W
N
285
200
175
20
interval D
b
th / tc
218.4 m
sn28.1
295
up/W
175
N
20
interval E
c
th / tc
226.5 m
sn25.1
up/W
N
285
200
20
interval F
d
th / tc
233.5 m
sn03.1
200
175
up/W
285
N
100
interval G
e
th / tc
449.67 m
S26.1a
175
200
up/W
260
20
N
interval I
f
th / tc
472.67 m
S32.1a
up/W
20
260
175
N
interval J
g
af / tc
26.6 m
sn87.2
20
up/W
N
50
100
0
interval A
h
af / tc
62.6 m
sn93.1
up/W
N
100
40
15
10
interval B
i
af / tc
170.05 m
sn70.1
10
up/W
25
50
Z
0
interval C
j
af / tc
279.58 m
SN_08_70.1
up/W
N
50
25
10
0
interval H
k
af / tc
267.94 m
SN_08_43.1
up/W
N
interval H
l

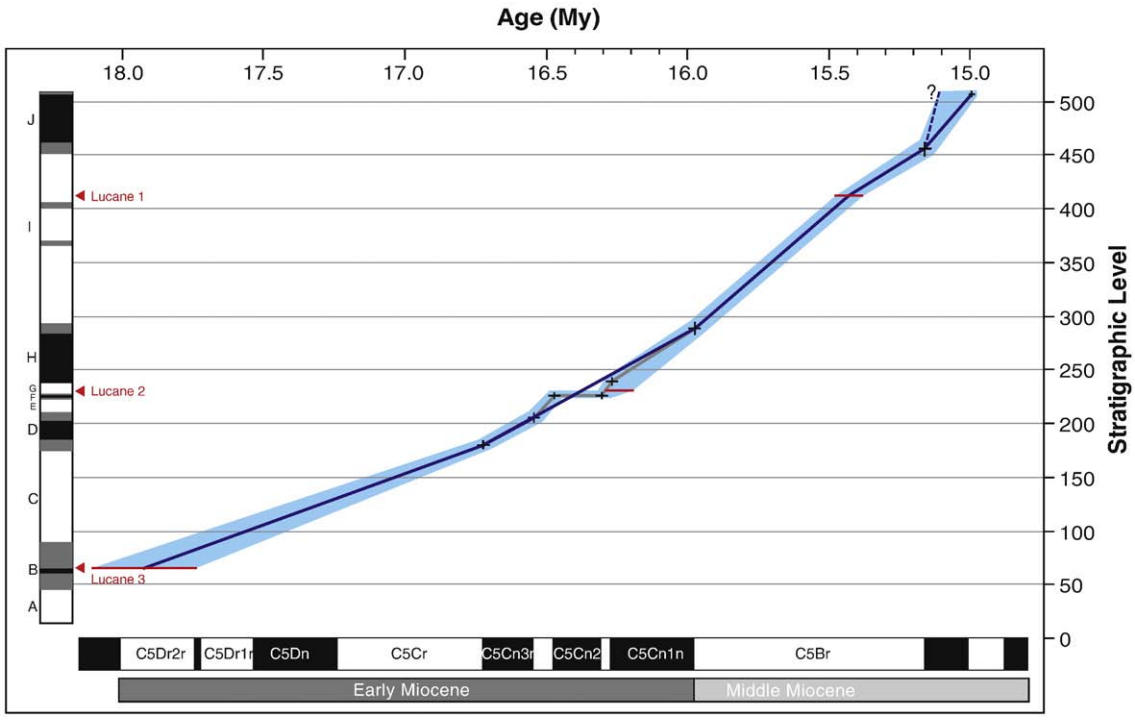

Fig. 7. Sedimentation rate along the Lučane section as derived from the constructed time-frame. In the lower half of the section the average rate is around 10 cm/ky while in upper half rates increase to about 20 cm/ky.

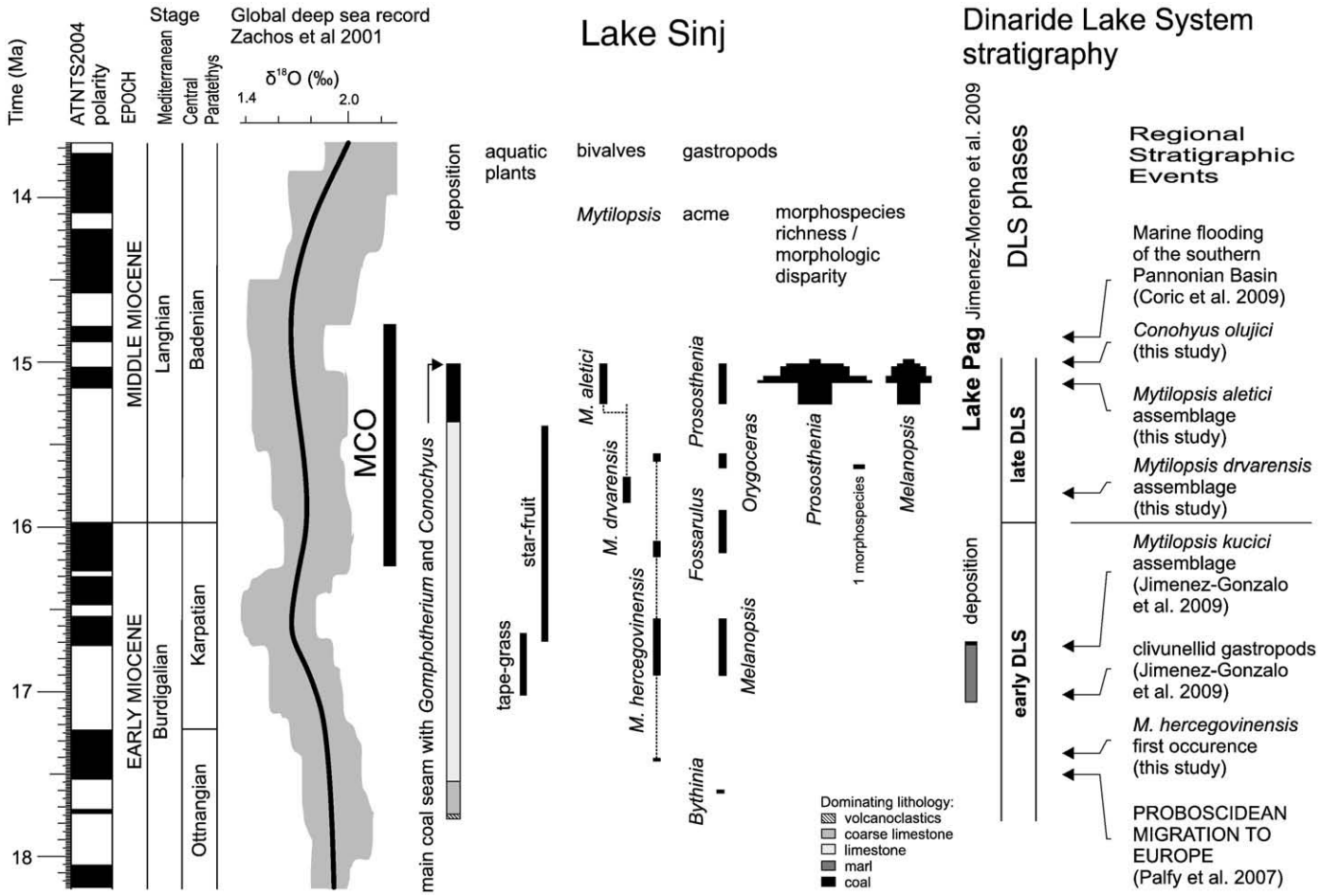

Fig. 8. New geochronology for the Lake Sinj deposits and fossil record correlated to an updated DLS stratigraphic model (geological time scale after Lourens et al., 2004; correlation of Central Paratethys stages after Piller et al., 2007; global climate record after Zachos et al., 2001).

this Lake Sinj occurrence is slightly younger than the corresponding Late Ottnangian horizon in the Alpine–Carpathian foredeep (Bůžek, 1982), which is approximately 17.5 Ma old according to Piller et al. (2007). These two *Doderleinia* horizons are thus apparently non-coeval, contrary to the hypothesis of Meller and Bergen (2003).

In the middle part of the investigated succession the tape-grass plant assemblage is suddenly replaced by a fossil star-fruit (*Damasonium*) assemblage (Fig. 8). Star-fruit remains are especially common in the upper part of that interval, corresponding to Zone 7 of the Kerner (1905b) lithostratigraphic division (Fig. 3) and now dated at ~15.5 Ma (Fig. 8). Based on recent star-fruit distribution and behavior, their mass occurrence in Lake Sinj has been tentatively related to intermittent acidification events bound to lake level rises inducing increased reworking of shore face material (Mandic et al., 2009).

The topmost part of the section, corresponding to Zone 8 of Kerner (1905b), is marked by a distinct palaeoenvironmental shift triggering enhanced production and preservation of organic matter as indicated by numerous lignite intercalations. This interval is now shown to represent the period between ~15.4 and ~15 Ma. The corresponding pollen spectrum (Jiménez-Moreno et al., 2008) is dominated by warm taxa with *Engelhardia* (walnut related tree plant), indicating a subtropical humid climate. The deposition of the lignites and its associated warm floral assemblage were probably induced by the advance of the Miocene Climatic Optimum (Fig. 8).

6.3. Age of the large mammal sites Lučane and Ruduša

The first evidence of long-term emersion of Lake Sinj is the 2 m thick coal seam in the uppermost part of the section. Its petrology (Mandic et al., 2009) suggests that the coal seam formed in a mire environment, which is corroborated by the recovery of several large land mammal fossils. Amongst these are the elephant-like proboscidean *Gomphoterium angustidens* (Cuvier) and the extinct pig *Conohyus olujici* (Olujić, 1999; Bernor et al., 2004). Remains of the extinct rhinoceros *Brachypotherium brachypus* (Latret) (Olujić, 1999) were excavated at a slightly higher stratigraphic level within the same coal bearing lithostratigraphic unit, exposed in the abandoned coal mine of Ruduša (Fig. 2). Both large mammal sites, previously tentatively estimated to be of late Early Miocene age (Bernor et al., 2004), are now shown to be ~15 Ma old. This age is in agreement with the age ranges of the represented vertebrate species that were, except for *C. olujici,* widely distributed throughout Europe and Asia Minor (Rössner and Heissig, 1999).

Cladistic analysis of *Conohyus olujici* by Bernor et al. (2004) showed it to be a very early member of the *Conohyus* clade, occurring prior to the clades striking radiation in Europe and South Asia. Its age was therefore estimated to range between 16–17 Ma. van der Made and Morales (2003) provided a review on *Conohyus* occurrences in Europe. According to their work, the earliest *Conohyus* remains (*C. simorrensis*) were found in at the localities Puente de Vallecas, Somosaguas and Montejo de la Vega in Spain, Hommes and Channay in France, Göriach, Au, St. Oswald and Rosenthal in Austria, Mala Miliva in Serbia, and Bâlâ in Turkey. They placed all these sites in zone E of the Iberian regional mammal zonation, which correlates to the topmost of MN5 of the European Mammal Zonation. Because, the base of zone E correlates with the base of the chron C5ACr (Krijgsman et al., 1994), the maximum numerical age for these *C. simorrensis* occurrences is 14.1 Ma. Our age model confirms the hypothesis of Bernor et al. (2004) that the ~15 Ma old extant pig of Lučane is the oldest *Conohyus* representative in Europe, even though the age for the Lučane site is more than 1 Myr younger than previously estimated.

The new age for *Conohyus olujici* does not support the inference by Bernor et al. (2004) that it is more primitive, i.e. older, than the earliest South Asian *Conohyus* (*C. sindiensis*). This could, however, be an artifact of conflicting stratigraphic data with regards to the first occurrence (FO) of *Conohyus* in South Asia. In the magnetostratigraphically dated Chita Parwela section (Johnson et al., 1985) of the Siwaliks (Pothohar/Potwar Plateau, Pakistan) the FO of *Conohyus* is recorded at 14.5 Ma (Barry in Bernor et al., 2004). In the Sehwan Section (Sind, Pakistan), on the other hand, *C. sindiensis* was recovered from a horizon that correlates biochronologically to a much older level (16.1 Ma) of the Chita Parwela section (De Bruijn and Hussain, 1984, Bernor et al., 1988). That correlation might on the other hand be ambiguous because Khan et al. (1984) assign the base of the Sehwan section to chron C5Bn.1r on the basis of their palaeomagnetic data. The whole succession would then be younger than 15 Ma (Hüsing, 2008). Flynn et al. (1995), in turn, report the FO of *Conohyus* in the Siwaliks at 16.3 Ma, which is distinctly older than the occurrence date at Lučane. We conclude that a thorough revision of the stratigraphic data of Pakistan is needed to solve these discrepancies.

6.4. Patterns in the mollusk fauna

A thorough literature investigation (Harzhauser and Mandic, 2008, 2010 and own data) shows that approximately 200 species and subspecies have been described from the Dinaride Lake System. About 110 are also reported to be present in the deposits of Lake Sinj. Lake Sinj and Lake Drniš (with its famous locality Miočić — Neumayr, 1869) together represent the classical malacological fossil site complex called the Dalmatian freshwater Neogene (e.g. Brusina, 1897). Despite its long tradition and apparent importance in palaeontological investigation no reliable age information was obtained so far. Numerous correlations resulted in multiple age inferences ranging from early Miocene (Bernor et al., 2004) through middle and late Miocene (Kochansky-Devidé and Slišković, 1978; Olujić, 1999) to Pliocene (Ivanović et al., 1977). Our study shows that the Lake Sinj sediments accumulated between 18 and 15 Ma.

The taxonomic richness of Lake Sinj and the DLS has no other Miocene counterpart in Europe, except for Lake Pannon (Harzhauser and Mandic, 2008). The DLS and Lake Pannon both show higher diversities than the modern ancient Lake Baikal, Lake Tanganyika or Lake Ohrid. For Lake Pannon this has been explained by its size and longevity that facilitated accumulation of species through iterative radiations and extinction events (Harzhauser and Mandic, 2010). It is now clear that Lake Sinj, with its extraordinary taxonomic richness and conspicuous endemic faunal character with up to 98% species elsewhere unknown (Harzhauser and Mandic, 2008) (Fig. 8) was a perennial aquatic environment that persisted for 3 Myr. Therefore, it can be inferred once more, that longevity enhanced the accumulation of taxa and resulted in striking patterns of autochthonous evolution.

Insight in the mechanism by which and especially the rate at which species diversity can increase arises from the uppermost part of the studied section, which corresponds to the time interval between 15.25 and 15 Ma. Here Olujić (1936, 1999) documents radiation events in two aquatic gastropod genera *Melanopsis* and *Prososthenia* (Fig. 8). These striking morphological disparity events are now shown to take place in ~100 kyr. Over this short course of time, two *Melanopsis* and six *Prososthenia* clades produced 28 transitional morphospecies. At the end of the radiation pulse, of both genera only one single species remained present in the lake. Which physical factor forced this course of evolutionary change is still a matter of investigation. The collection of additional data and geochemical proxies in particular is necessary to resolve this issue.

The original uncertainty about the age of the DLS did not allow an accurate interpretation of its palaeobiogeographic relation to Lake Pannon. Our study shows that deposition in Lake Sinj had ended 3 Myr before deposition in Lake Pannon commenced. Whereas some endemic genera such as *Orygoceras* managed to survive in the region until the rise of the Lake Pannon, the lack of similarity at species level already suggested a certain disconnection between these two domains (Harzhauser and Mandic, 2008).

One important aspect of the present study was the calibration of the evolutionary trends in mollusk fauna to the global timescale for the purpose of regional biostratigraphic correlation. Fig. 8 displays the occurrences and local acmes of mollusk species over the course of time as recorded in the studied section. Dreissenid bivalves (*Mytilopsis*) are especially important for regional correlation since they show striking evolutionary changes and are common throughout the Dinaride Lake System (Kochansky-Devidé and Slišković, 1978, 1980). In the Lučane section, the occurrence of one small and primitive *Mytilopsis* (*M. hercegovinensis*) is restricted to the lower and middle part, whereas the larger and more advanced *M. drvarensis* and *M. aletici* are traced throughout the middle and the upper part. According to our new results, the morphological transition between *M. drvarensis* and *M. aletici*, characterized by an increase in size and flattening of the shell (cf. Mandic et al., 2009), occurred between 15.25 and 15.7 Ma and took less than 450 kyr (Fig. 8).

When combined with the previously established age calibration of the occurrence of *M. kucici* and clivunellid gastropods in Lake Pag (Jiménez-Moreno et al., 2009; Bulić and Jurišić-Polšak, 2009) (Fig. 8) these results prove the hypothesis of Kochansky-Devidé and Slišković (1978) that the younger strata of the DLS are characterized by the presence of highly evolved endemics such as *M. aletici*, whereas the older parts bear clivunellid gastropods and significantly more primitive dreissenids. This allows us to correlate the stratigraphic boundary between the early and late DLS phase, which slightly precedes the first occurrence of *M. drvarensis*, with the base of chron C5Br.

In the north-eastern part of the DLS, lacustrine strata lack the highly evolved mollusk fauna with *M. drvarensis* and *M. aletici* so characteristic for Lake Sinj, and are superposed by marine Badenian Paratethys sediments. Kochansky-Devidé and Slišković (1978) therefore hypothesized that the region wide marine incursion occurred before *M. drvarensis* and *M. aletici* evolved. The lowermost marine strata have, however, lately been dated at 14.8 Ma by means of marine plankton stratigraphy (Ćorić et al, 2009). Lacustrine sedimentation in the Sinj basin thus preceded the flooding of the northern parts of the DLS by the Paratethys Sea and the hypothesis of Kochansky-Devidé and Slišković must be abandoned. A different explanation for the exclusive occurrence of the higher evolved mollusk assemblage in the southern DLS has thus to be found. Such evaluation, which must be based on the complete DLS record, is beyond the scope of the present study.

7. Conclusions

The combined palaeomagnetic and $^{40}Ar/^{39}Ar$ data presented in this paper allow correlation of the lacustrine succession deposited in Lake Sinj to the global timescale. Thereby, Lake Sinj becomes the first of the Miocene Dinaride Lakes to be accurately dated. It is now clear that its deposits accumulated from 18 to 15.0 Ma, which correlates to the upper Burdigalian and lower Langhian Mediterranean stages and Ottnangian, Karpatian and lowermost Badenian Paratethys stages.

The evolutionary model for dreissenid radiation across the Dinaride Lake System has been significantly improved since the timing of several acme occurrences in the studied section could be established. We confirm the relative stratigraphic positions previously derived from regional stratigraphic patterns and evolutionary relationships inferred from shell morphologies (Kochansky-Devidé and Slišković (1978, 1980)). Moreover, an exact biochronology of acme ranges for three marker species is established: the primitive long-lived universalist *Mytilopsis hercegovinensis* from 17.4 to 15.6 Ma, the intermediate *M. drvarensis* from 15.9 to 15.7 Ma and finally the crown of Dinaride Lake autochthonous evolution, the highly progressive specialist *M. aletici* from 15.3 to 15.0 Ma.

According to our results, the *Conohyus olujici* mandibles preserved at the very top of the investigated Lučane section have an absolute age of 15.0 Ma. Although this is much younger than the age estimate of 16–17 Ma by Bernor et al. (2004) it still makes *C. olujici* the oldest *Conohyus* in Europe.

It is evident that the integration of palaeomagnetic and $^{40}Ar/^{39}Ar$ research provides a powerful method to date sedimentary successions, like those of Lake Sinj, plagued by endemism. It furthermore presents a straightforward method to improve palaeogeographic reconstructions for the Dinaride Lake System as a whole.

Acknowledgements

"We are grateful to the Austrian FWF Project P18519-B17: Mollusk Evolution of the Neogene Dinaride Lake System", and we acknowledge support by The Netherlands Research Centre for Integrated Solid Earth Sciences (ISES) and by The Netherlands Organization for Scientific Research (NWO). In addition, we would like to thank Roel van Elsas for his help with the mineral separation and Tom Mullender and Mark Dekkers for their help with the palaeomagnetic measurements. Finally, we would like to thank both Miguel Garcés and an anonymous reviewer for their constructive comments.

Appendix A. Supplementary data

Supplementary data associated with this article can be found, in the online version, at doi:10.1016/j.palaeo.2010.03.040.

References

Bernor, R.L., Flynn, L.J., Harrison, T., Hussain, S.T., Kelley, J., 1988. Dionysopithecus from southern Pakistan and the biochronology and biogeography of early Eurasian catarrhines. Journal of Human Evolution 17, 339–358.
Bernor, R., Bi, S., Radovčić, J., 2004. A contribution to the evolutionary biology of *Conohyus olujici* n. sp. (Mammalia, Suidae, Tetraconodontinae) from the early Miocene of Lučane, Croatia. Geodiversitas 26, 509–534.
Billups, K., Pälike, H., Channell, J.E.T., Zachos, J., Shackleton, N.J., 2004. Astronomic calibration of the late Oligocene through early Miocene geomagnetic polarity time scale. Earth and Planetary Letters 224, 33–44.
Brusina, S., 1874. Fossile Binnen–Mollusken aus Dalmatien, Kroatien und Slavonien nebst einem Anhange. Actienbuchdruckerei, Agram, p. 138.
Brusina, S., 1884. Die Neritodonta Dalmatiens und Slavoniens nebst allerlei malakologischen Bemerkungen. Jahrbücher der Deutschen Malakozoologischen Gesellschaft, 11, pp. 17–120. Frankfurt am Main.
Brusina, S., 1897. Gragja za neogensku malakološku faunu Dalmacije, Hrvatske i Slavonije uz neke vrste iz Bosne i Hercegovine i Srbije. Djela Jugoslavenske akademije znanosti i umjetnosti, 18, pp. 1–43. Zagreb.
Brusina, S., 1902. Ichonographia molluscorum Fossilium in telure tertiaria Hungariae. Croatie, Slavoniae, Bosniae etc., 30 Taf., Zagreb.
Bulić, J., Jurišić-Polšak, Z., 2009. The lacustrine miocene deposits at Crnika beach on the island of Pag (Croatia). Geologia Croatica 62 (3), 135–156.
Bůžek, Č., 1982. *Ceratostratiotes gregor*, an extinct water plant of uncertain affinity from the European Miocene. Věstník Ústředního ústavu geologického 57 (5), 285–294 Prague.
Ćorić, S., Pavelić, D., Rögl, F., Mandic, O., Vrabac, S., Avanić, R., Jerković, L., Vranjković, A., 2009. Revised Middle Miocene datum for initial marine flooding of North Croatian Basins (Pannonian Basin System, Central Paratethys). Geologica Croatica 62 (1), 31–43.
De Bruijn, H., Hussain, S.T., 1984. The succession of rodent faunas from the Lower Manchar Formation southern Pakistan and its relevance for the biostratigraphy of the Mediterranean Miocene. Paléobiologie continentale 14, 191–204.
Flynn, L.J., Barry, J.C., Morgan, M.E., Pilbeam, D., Jacobs, L.L., Lindsay, E.H., 1995. Neogene Siwalik mammalian lineages: species longevities, rates of change, and modes of speciation. Palaeogeography Palaeoclimatology Palaeoecology 115, 249–264.
Gorthner, A., 1994. What is an ancient lake? In: Martens, K., Goddeeris, B., Coulter, G. (Eds.), Speciation in Ancient Lakes. Archiv für Hydrobiologie: Beiheft. Ergebnisse der Limnologie, 44, pp. 97–100.
Harzhauser, M., Mandic, O., 2008. Neogene lake systems of Central and South-Eastern Europe: faunal diversity, gradients and interrelations. Palaeogeography, Palaeoclimatology, Palaeoecology 260, 417–434.
Harzhauser, M., Mandic, O., 2010. Neogene dreissenids in Central Europe: evolutionary shifts and diversity changes, In: van der Velde, G., Rajagopal, S., bij de Vaate, A. (Eds.), The Zebra Mussel in Europe, Chapter 2. Backhuys Publishers, Leiden/Margraf Publishers, Weikersheim, pp. 11–29. 555 pp.
Hüsing, S., 2008. Astrochronology of the Mediterranean Miocene: Linking palaeoenvironmental changes to gateway dynamics (PhD Thesis Utrecht University), Geologica Ultraiectina, 295, 171 pp.
Ivanović, A., Sikirica, S., Marković, S. and Sakač, K. 1977. Osnovna geološka karta SFRJ, List Drniš L 33-141. 1:100.000. - Savezni geološki zavod, Beograd.

Jiménez-Moreno, G., Mandic, O., Harzhauser, M., Pavelić, D., Vranjković, A., 2008. Vegetation and climate dynamics during the early Middle Miocene from Lake Sinj (Dinaride Lake System, SE Croatia). Review of Palaeobotany and Palynology 152, 237–245.

Jiménez-Moreno, G., de Leeuw, A., Mandic, O., Harzhauser, M., Pavelić, D., Krijgsman, W., Vranjković, A., 2009. Integrated stratigraphy of the early Miocene lacustrine deposits of Pag Island (SW Croatia): palaeovegetation and environmental changes in the Dinaride Lake System. Palaeogeography, Palaeoclimatology, Palaeoecology 280, 193–206.

Johnson, N.M., Stix, J., Tauxe, L., Cerveny, P.F., Tahirkheli, R.A.K., 1985. Paleomagnetic chronology, fluvial processes, and tectonic implications of the Siwalik deposits near Chinji village, Pakistan. The Journal of Geology 27–40.

Kerner, F., 1905a. Neogenpflanzen vom Nordrande des Sinjsko polje in Mitteldalmatien. Jahrb Geol RA 593–612.

Kerner, F., 1905b. Gliederung der Sinjaner Neogen-formation. Verhandl. Geol. Reichanst 127–165.

Kerner, F., 1916a. Sinj und Spalato 1:75.000/neu aufgenommen und bearbeitet in den Jahren 1902–1909.

Kerner, F., 1916b. Erläuterungen zur Geologischen Karte der Österr.- Ungarn. Monarchie 1:75.000, Sinj und Spalato. Wien : Geologische Reichsanstalt.

Khan, M., Hussain, S., Arif, M., Shaheed, H., 1984. Preliminary paleomagnetic investigations of the Manchar Formation, Gaj River section, Kirthar Range. Geological bulletin, Pakistan.

Kirschvink, J.L., 1980. The least-squares line and plane and the analysis of palaeomagnetic data. Geophysical Journal International 62, 699–718.

Kittl, E., 1895. Bericht über eine Reise in Norddalmatien und einem angrenzenden Theile Bosniens. Ann. d. k. k. Naturhist. Hofmuseums 10, 91–96.

Kochansky-Devidé, V., Slišković, T., 1978. Miocenske Kongerije Hrvatske, Bosne i Hercegovine (Miozäne Kongerien von Kroatien, Bosnien und Herzegowina). Paleontol. Jugosl. 19, 1–98.

Kochansky-Devidé, V., Slišković, T., 1980. Mlađe miocenske Kongerije Livanjskog, Duvanjskog i Kupreškog polja u jugozapadnoj Bosni i Hodova u Hercegovini. Palaeontologia Jugoslavica 25, 1–25.

Koppers, A.A.P., 2002. ArArCALC—software for 40Ar/39Ar age calculations. Computers and Geosciences 28, 605–619.

Krijgsman, W., Langereis, C.G., Daams, R., Van der Meulen, A., 1994. Magnetostratigraphic dating of the middle Miocene climate change in the continental deposits of the Aragonian type area in the Calatayud–Teruel basin (Central Spain). Earth Planet. Sci. Lett. 128, 513–526.

Krstić, N., Dumurdžanov, N., Olujić, J., Vujnović, L., Janković-Golubović, J., 2001. Interbedded tuff and bentonite in the Neogene lacustrine sediments of the Balkan Peninsula. A review. Acta Vulcanologica 13, 91–100.

Krstić, N., Savić, L., Jovanović, G., Bodor, E., 2003. Lower Miocene lakes of the Balkan Land. Acta Geologica Hungarica 46, 291–299.

Kuiper, K.F., Deino, A., Hilgen, F.J., Krijgsman, W., Renne, P.R., Wijbrans, J.R., 2008. Synchronizing rock clocks of Earth history. Science 320, 500.

Lanci, L., Pares, J.M., Channell, J.E.T., Kent, D.V., 2004. Miocene magnetostratigraphy from Equatorial Pacific sediments (ODP Site 1218, Leg 199). Earth and Planetary Science Letters 226, 207–224.

Larrasoaña, J.C., Murelaga, X., Garcés, M., 2006. Magnetobiochronology of Lower Miocene (Ramblian) continental sediments from the Tudela Formation (western Ebro basin, Spain). Earth and Planetary Science Letters 243 (3–4), 409–423.

Lourens, L.J., Hilgen, F.J., Shackleton, N.J., Laskar, J., Wilson, D., 2004. The Neogene Period. A Geologic Time Scale 2004, 409–440.

Mandic, O., Pavelić, D., Harzhauser, M., Zupanič, J., Reischenbacher, D., Sachsenhofer, R.F., Tadej, N., Vranjković, A., 2009. Depositional history of the Miocene Lake Sinj (Dinaride Lake System, Croatia): a long-lived hard-water lake in a pull-apart tectonic setting. Journal of Paleolimnology 41, 431–452.

Marinčić, S., Korolija, B., Majcen, Z., 1969. Omiš.-Osnovna Geološka Karta SFRJ 1:100000, (VGI) Beograd.

Marinčić, S., Korolija, B., Mamužić, N., Magaš, Z., Majcen, Z., Brkić, M., Benček, D., 1977. Tumač za list Omiš. - Osnovna Geološka Karta SFRJ 1:100000, (VGI) Beograd.

McDougall, I., Harrison, T.M., 1999. Geochronology and Thermochronology by the 40Ar/39Ar Method. Oxford University Press, USA.

Meller, B., Bergen, P.F.v., 2003. The problematic systematic position of Ceratostriatus Gregor (Hydracharitaceae ?) — morphological, anatomocal and biochemical comparison with Stratiotes L. Plant Systematics and Evolution 236, 125–150.

Neumayr, M., 1869. Beiträge zur Kenntniss fossiler Binnenfaunen. Jahrbuch der kaiserlichen und königlichen geologischen Reichsanstalt 19, 355–382 Wien.

Olujić, J., 1936. Ueber die geschlossenen, progressiven Entwicklungsreihen der Schalen der pontischen Prososthenien (Vorläufige Mitteilung). Arch Molluskenkd 68, 118–120.

Olujić, J., 1999. O razvojnim nizovima nekoliko melanopsida i prozostenida iz sarmatskih naslaga okolice Sinja (Dalmacija, Hrvatska). In: Olujić, J. (Ed.), O razvojnim nizovima nekoliko melanopsida i prozostenida iz sarmatskih naslaga okolice Sinja (Dalmacija, Hrvatska). — pp. 7–32 + 33–60 p., (Hrvatski prirodoslovni muzej) Zagreb and (Provincijalat Franjevačke provincije presvetog Otkupitelja) Sinj.

Pálfy, J., Mundil, R., Renne, P.R., Bernor, R.L., Kordos, L., Gasparik, M., 2007. U–Pb and $^{40}Ar/^{39}Ar$ dating of the Miocene fossil track site at Ipolytarnóc (Hungary) and its implications. Earth and Planetary Science Letters 258, 160–174.

Papeš, J., Magaš, N., Marinković, R., Sikirica, V., Raić, V., 1982. Sinj. — Osnovna Geološka Karta SFRJ 1:100000, (VGI) Beograd.

Pavelić, D., 2002. The south-western boundary of Central Paratethys. Geologia Croatica 55, 83–92.

Pérez-Rivarés, F.J., Garcés, M., Arenas, C., Pardo, G., 2004. Magnetostratigraphy of the Miocene continental deposits of the Montes de Castejón (central Ebro basin, Spain): geochronological and paleoenvironmental implications. Geologica Acta 2 (3), 221–234.

Piller, W.E., Harzhauser, M., Mandic, O., 2007. Miocene Central Paratethys stratigraphy — current status and future directions. Stratigraphy 4, 151–168.

Raić, V., Papeš, J., Sikirica, V., Magaš, N., 1984. Tumač za list Sinj K 33–10. Osnovna Geološka Karta SFRJ 1:100000, pp. 1–48, (Savezni geološki zavod) Beograd.

Rasser, M., Harzhauser, M., Anistratenko, V., Bassi, D., Belak, M., Berger, J., Bianchini, G., Čićić,, S., Čosović, V., Dolakova, N., 2008. Palaeogene and Neogene. The Geology of Central Europe: Mesozoic and Cenozoic 1031.

Rögl, F., Ćorić,, S., Daxner-Höck, H., Harzhauser, M., Mandic, O., Svábenická, L., Zorn, I., 2004. Correlation of the Karpatian Stage. The Karpatian — A Lower Miocene Stage of the Central Paratethys. Masaryk University, Brno, pp. 27–34.

Rössner, G., Heissig, K., 1999. The Miocene Land Mammals of Europe. Pfeil, München. 516 pp.

Schmid, S.M., Bernoulli, D., Fügenschuh, B., Matenco, L., Schefer, S., Schuster, R., Tischler, M., Ustaszewski, K., 2008. The Alpine–Carpathian–Dinaridic orogenic system: correlation and evolution of tectonic units. Swiss Journal of Geosciences 101, 139–183.

Steiger, R.H., Jäger, E., 1977. Subcommission on geochronology: convention on the use of decay constants in geo-and cosmochronology. Earth and Planetary Science Letters 36, 359–362.

Šušnjara, A., Sakač, K., 1988. Miocene freshwater sediments of the Sinj area—Middle Dalmatia. Geološki vjesnik 41, 51–74.

Šušnjara, A., Šćavničar, B., 1974. Tuffs in Neogene deposits of Central Dalmatia (Southern Croatia). Geol. Vjesn 27, 239–253.

Takšić, A., 1968. Die Vertebratenfauna aus dem Goručicatal bei Sinj. Bull. Sci. Cons. Acad. Yougosl., A 13 (3–4), 74–75 Zagreb.

Tari-Kovačić, V., 1994. The role of palaeogene clastics in the tectonic interpretation of Northern Dalmatia. Geologia Croatica 47, 127–138.

Tari-Kovačić, V., 2002. Evolution of the northern and western Dinarides: a tectonostratigraphic approach. Stephan Mueller Special Publication Series 1, 223–236.

van der Made, J., Morales, J., 2003. The pig *Conohyus simorrensis* from the upper Aragonian of Alhamibra, Madrid, and a review of the distribution of European Conohyus. Estudios Geológicos 59.

Zachos, J., Pagani, M., Sloan, L., Thomas, E., Billups, K., 2001. Trends, rhythms, and aberrations in global climate 65 Ma to present. Science 292, 686–693.

Zijderveld, J., 1967. A.c. demagnetisation of rocks: analysis of results. Methods in Palaeomagnetism. Elsevier, Amsterdam, pp. 254–286.